Proceedings of the 2009 IEEE International Conference on Systems, Man, and Cybernetics
San Antonio, TX, USA - October 2009

A Microfluidic Electroosmotic Mixer and the Effect of Potential and Frequency on its Mixing Efficiency

A. Z. Kouzani, K. Khoshmanesh
School of Engineering
Deakin University
Geelong, VIC 3217, Australia
kouzani, kkho@deakin.edu.au

S. Nahavandi
Centre for Intelligent Systems Research
Deakin University
Geelong, VIC 3217, Australia
nahavand@deakin.edu.au

J. R. Kanwar
BioDeakin
Deakin University
Geelong, VIC 3217, Australia
jagat.kanwar@deakin.edu.au

***Abstract*—This paper presents the design and numerical simulation of a T-shape microfluidic electroosmotic micromixer. It is equipped with six microelectrodes that are embedded in the side surfaces of the microchannel. The electrode array consists of two sets of three 20 µm and 60 µm microelectrodes arranged in the form of two opposing triangles. Numerical analysis of electric potential and frequency effects on mixing efficiency of the micromixer is carried out by means of two sets of simulations. First, the electric potential is kept at 2 V while the frequency is varied within 10-50 Hz. The highest achieved mixing efficiency is 96% at 22 Hz. Next, the frequency is kept at 30 Hz whilst the electric potential is varied within 1-5 V. The best achieved mixing efficiency is 97% at 3 V.**

***Keywords*—microfluidics, micromixer, electroosmotic flow, mixing efficiency**

I. INTRODUCTION

In recent years, development of microfluidic lab-on-a-chip systems has provided opportunities to create novel self-regulated implantable drug delivery systems to maximise the efficiency of drug therapies. Fluid mixing is an important task that is incorporated in a microfluidic drug delivery system.

Fluid mixing in microfluidic devices [1] is typically influenced by diffusion phenomenon. Micromixers are therefore employed to enhance the mixing rate in different flow rates within a wide range of physical characteristics of bio-particles and solutions. The micromixers can be generally categorised into two groups: passive and active. In passive mixers, neither moving parts nor energy injectors are utilised. In active mixers, on the other hand, an actuator or an energy source is employed to agitate the solution.

Electrokinetics [2] generally involves the study of liquid or particle motion under the action of an electric field. It includes electroosmosis, electrophoresis, dielectrophoresis, and electro-wetting. Electroosmotic flow is a method for mixing in microfluidic and nanofluidic systems. Electrodes are incorporated in these devices in order to agitate the solution. Electrokinetic micromixers have been discussed in [2-5].

This paper presents the design and numerical simulation of a T-shape microfluidic electroosmotic micromixer equipped with six microelectrode arrays. Numerical analysis of electric potential and frequency effects on mixing efficiency of the micromixer is carried out by means of two sets of simulations. The results are presented and discussed.

The paper is organised as follows. Section II presents the formulas governing the problem. Section III describes principles of the proposed micromixer, its geometry, and the governing equation. Section IV describes the simulation results, presents the calculated mixing efficiencies, and discusses the performance of the mixromixer under various electric potentials and frequencies. Finally, the concluding remarks are given in Section V.

II. THEORETICAL CONCEPTS

The motion of the mixing fluids is governed by the equations of continuity and momentum, as given below. Here, the momentum equation contains a source term, which imposes the electroosmotic forces to the flow:

$$\nabla \cdot \vec{V} = 0 \tag{1}$$

$$\rho \frac{\partial \vec{V}}{\partial t} + \rho \vec{V} \cdot \nabla \vec{V} = -\nabla P + \mu \nabla^2 \vec{V} - \rho_e E \tag{2}$$

where V is velocity, t is time, P is pressure, ρ is density, μ is dynamic viscosity, and E is electric field. Here, ρ_e represents the charge density within the flow that is obtained from the following equation, [6-7].

$$\rho_e = \varepsilon_\circ \varepsilon \nabla^2 \psi \tag{3}$$

where $\varepsilon_\circ$ is the vacuum permittivity and ε is the relative permittivity of the fluid, and ψ is the local concentration of the electric potential within the flow. ψ is governed by the Poisson-Boltzman differential equation as below:

$$\nabla^2 \psi = \kappa^2 \psi \tag{4}$$

where κ is the Debye-Huckel parameter that is the inverse of the electric-double-layer (EDL). Solving this equation implies that ψ decays exponentionally getting off the microchannel surfaces as below:

$$\psi = \zeta_p \cdot \exp(-\kappa y) \tag{5}$$

978-1-4244-2794-9/09/$25.00 ©2009 IEEE

978-1-4244-2794-9/09/$25.00 ©2009 IEEE

where ζ_p is the zeta potential that determines the electric potential of the fluid at the microchannel surface. In this work, ζ_p is taken as -0.1 V.

Calculating the velocity field of the mixing flows, the local concentration of the species is obtained by solving the equation of mass transport, as given below:

$$\frac{\partial C}{\partial t} + \vec{V} \cdot \nabla C = D \nabla^2 C \qquad (6)$$

where C is the local concentration of species. Solving Equations (1-6), the distribution of velocity, pressure and concentration of species is obtained in the microchannel.

III. Proposed Micromixer

The proposed active mixer includes a T-shape microchannel, where two fluids enter the lower and upper 50 µm wide inlet channels, and then enter a 100 µm wide mixing channel. The mixing channel is equipped with six microelectrodes embedded in the surface of the microchannel. The electrode array consists of two sets of three 20 µm and 60 µm long microelectrodes that are arranged in two opposite triangles. More information about the geometry of microchannel and the configuration of the microelectrodes can be seen in Figure 1.

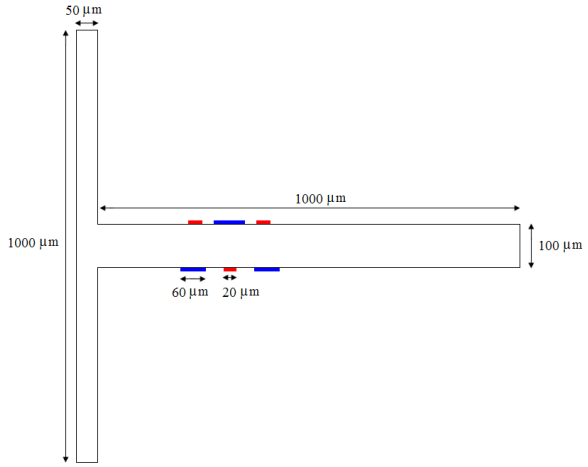

Figure 1. The geometry of the proposed micromixer.

Computational Fluid Dynamics (CFD) method is applied to simulate the micro-mixers. A number of 1479 unstructured elements were applied to discriticise the control volume of the micromixer , as shown in Figure 2. The density of the elements is constant alongside the channel walls and electrodes location, as well as within microchannel.

The physical properties of the fluids can be categorised into thermophysical and electrical. The thermophysical properties that are density, dynamic viscosity, and diffusion coefficient are selected as 10^3 kg/m^3, 10^{-3} Pa.s, and 10^{-11} m^2/s, respectively. The electrical properties that are conductivity and relative permittivity are chosen as 12×10^{-2} S/m, and 81, respectively. The flow enters the lower and upper inlets at 10^{-4} m/s. The concentration of the solution for the lower and the upper inlets are selected as 0 and 1 respectively.

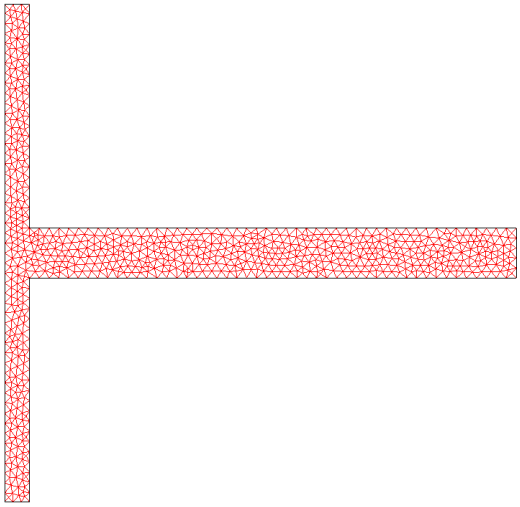

Figure 2. 1479 unstructured elements were applied to discriticise the control volume of the micromixer.

The frequency of the signal applied to the microelectrode array varies within 10 to 50 Hz, while the applied electric potential varies within 1 to 5 V. The 20 µm electrodes receive a negative polarity, while the 60 µm electrodes receive a positive polarity as shown in Figure 3.

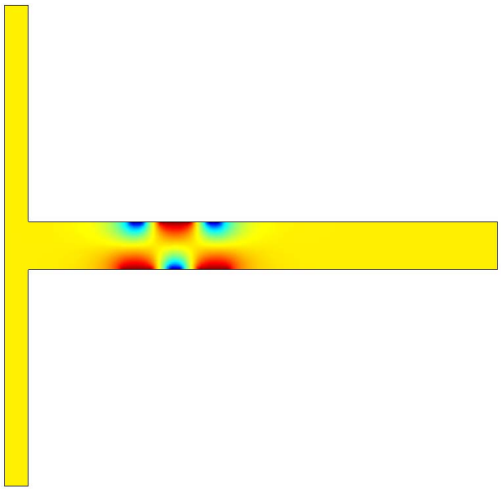

Figure 3. The 20 µm electrodes receive a negative potential while the 60 µm electrodes receive a positive potential. The magnitude of the electric potential at the displayed contour is 3 V across the electrodes.

IV. Numerical Simulations

In order to study the performance of the developed electroosmotic micromixer, two sets of experiments were carried out as described in the following.

A. Experiment 1

In the first set of experiments, the magnitude of the applied electric potential across the electrodes was kept constant at 2 V whilst the applied frequency was varied within the range of 10-50 Hz with a 10 Hz increment. Figure 4 displays the concentration distribution of the solution. The contours are coloured according to the concentration of the flow, with red as the maximum and blue as the minimum. The green corresponds to the middle concentration representing the perfect mixing.

The upper inlet is fed with maximum concentration while the lower one with minimum. Before the flow comes across the first electrode, the mixing is limited to the interface of the upper and the lower flows. At this region, the mixing is performed by pure diffusion, and a low mixing is resulted. Once the flow passes the first electrode, it is affected by the electroosmotic disturbances caused by the electric field. The induced instability is proportional to the applied frequency. At the frequency of 10 Hz, there is a poor mixing adjacent to the microchannel surfaces. Increscent of frequency resulted in an improvement of the mixing at the boundary layer regions of the micromixer.

B. Experimet 2

In the second set of experiments, the applied frequency was kept constant at 30 Hz whilst the applied electric potential was varied within the range of 1-5 V with a 0.5 V increment. Figure 5 illustrates the concentration distribution of the solution. The induced instability is proportional to the applied electric potential within 1 to 3 V. Increasing the magnitude of the electric potential beyond this range disturbs the mixing, as shown in the bottom image. The induced electric energy seems to be so great making the flow turbulent. In this case, the flow can no longer be simulated by the laminar form of Navier-Stokes equations.

In order to evaluate the performance of the electrokinetic instability micromixer, the mixing efficiency is calculated across the outlet port using the following equation:

$$\eta = \left(1 - \frac{\int_{outlet} \rho_e \, u_e \left| c_e - c_\infty \right| dA}{\int_{inlets} \rho_i \, u_i \left| c_i - c_\infty \right| dA} \right) \times 100\% \qquad (7)$$

where c_e, u_e, ρ_e are the concentration, velocity and density at the outlet port of the micro-channel, while c_i, u_i, and ρ_i are those at the inlets and c_∞ is the infinite fully mixed concentration.

The equation was basically introduced in [8]; however the mass fluxes are included in the integration to represent the velocity distribution across the mixing channel as proposed in [9]. In this manner, the middle regions of the channel appear more decisive compared to the boundary layer regions.

The mixing efficiencies that were calculated in the two set of experiments are depicted in Figures 6-7. Polynomial curves are fitted on the calculated values.

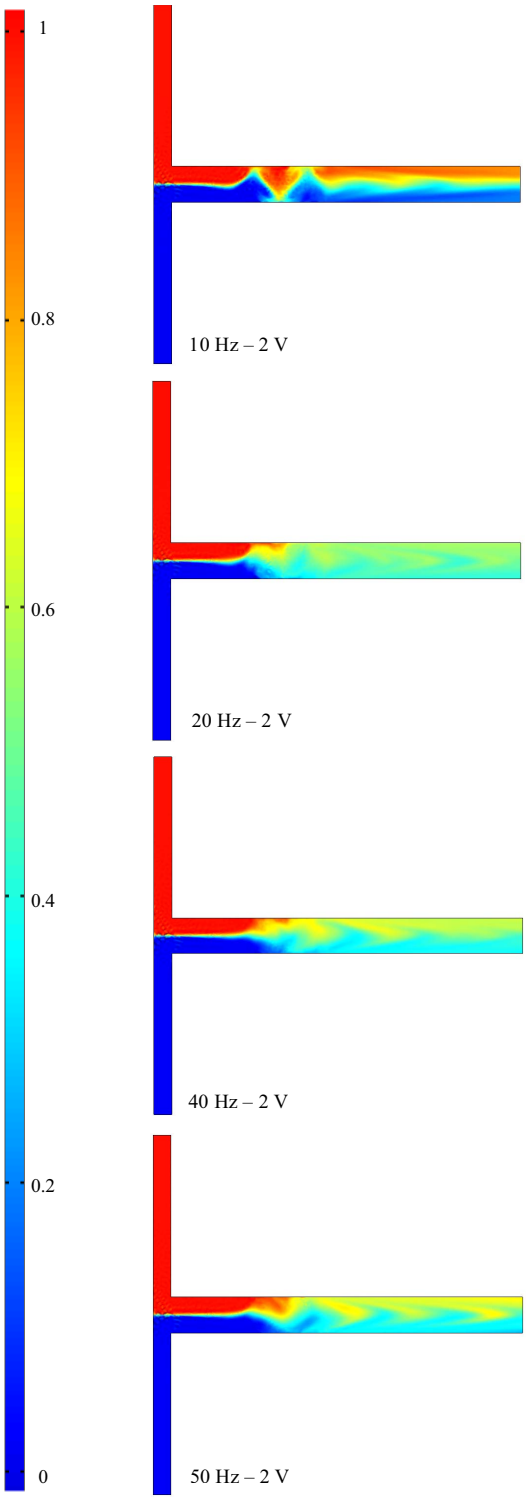

Figure 4. The concentration distribution of the solution under the constant electric potential of 2 V and the frequency range of 10-50 Hz.

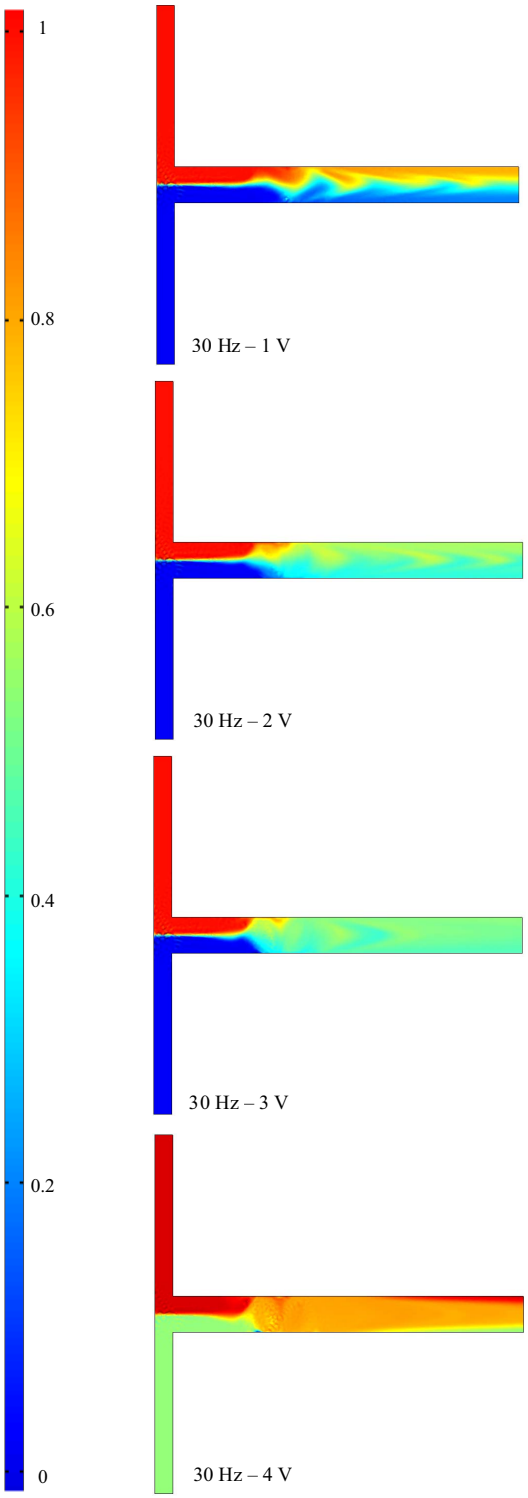

Figure 5. The concentration distribution of the solution under the constant frequency of 30 Hz and the electric potential range of 1-4 V.

Figure 6 illustrates the variations of the mixing efficiency for the first set of experiments. As can be seen, the mixing efficiency increases sharply within the range of 10 to about 22 Hz. It then decreases smoothly beyond the peak point at about 22 Hz. At this frequency, the mixing efficiency of 96% is achieved. This is because, at the specific electric potential of 2 V, the flow does not get enough time to absorb the disturbances of the frequencies beyond 22 Hz. It is why poor mixing is achieved at the boundary layer regions as shown in Figure 4.

Figure 7 shows the variations of the mixing efficiency for the second set of experiments. As can be seen, the mixing efficiency increases smoothly within the range of 1 to 3 V. As described before, increasing the electric potential beyond 3 V at the specific frequency of 30 Hz disturbs the flow field and the results are not physically explainable. The maximum mixing efficiency was found to be 97%.

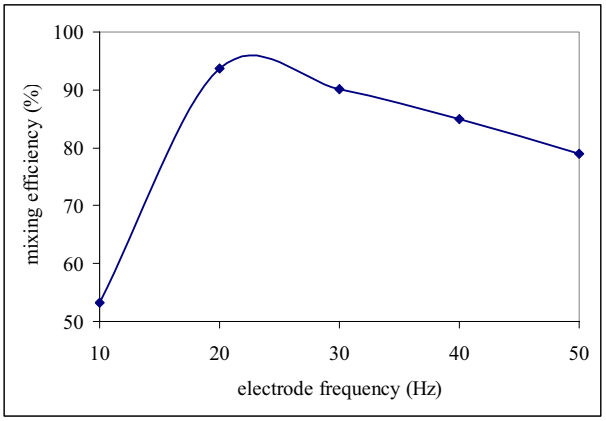

Figure 6. Variation of mixing efficiency over the frequency range of 10-50 Hz and the constant electric potential of 2 V, corresponding to Figure 4.

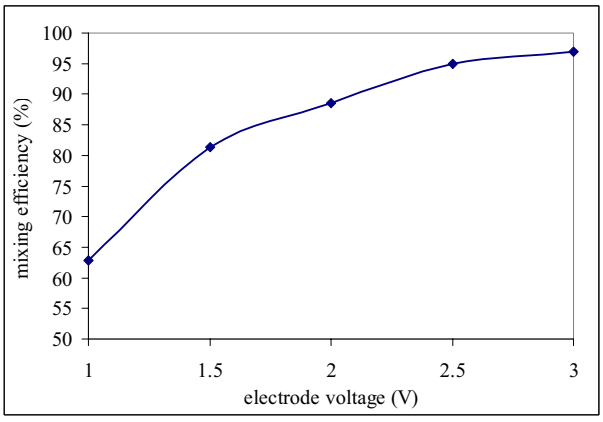

Figure 7. Variation of mixing efficiency over the electric potential range of 1-3 V and the constant frequency of 30 Hz, corresponding to Figure 5.

A direct comparison of the performance of the described work against similar existing electroosmotic micromixers was not possible due to the fact that the reported existing approaches have not been found carrying out numerical simulation to the extent performed in this study.

The achieved mixing efficiency is considered to be a good outcome for our micromixer that has a simple structure. The applications of such a micromixer are numerous. In particular, it can be employed as the microfluidic component of lab-on-a-chip systems.

V. Conclusions

An active electroosmotic micromixer that is equipped with six microelectrode array was presented in this paper. The electrode array includes a set of three 20 μm and a set of three 60 μm long microelectrodes. The 20 μm electrodes receive a negative potential while the 60 μm electrodes receive a positive potential. The behaviour of flow was simulated by means of the computational fluid dynamics method. Two sets of experiments were carried out. First, the magnitude of the applied electric potential across the electrodes was kept at 2 V whilst the applied frequency was varied within 10-50 Hz. The mixing efficiency increased sharply within the range of 10 to about 22 Hz, then decreased smoothly beyond 22 Hz. At 22 Hz, the mixing efficiency was 96%. Next, the applied frequency was kept constant at 30 Hz whilst the applied electric potential was varied within 1-5 V. The mixing efficiency increases smoothly within the range of 1 to 3 V. Beyond 3 V at 30 Hz the flow field is disturbed. The maximum mixing efficiency achieved was 97%. The mixromixer possesses a simple structure and is affordable justifying its usability in lab-on-a-chip devices for various medical purposes.

References

[1] C. Yi, C.-W. Li, S. Ji, and M. Yang, "Microfluidics technology for manipulation and analysis of biological cells," Analytica Chimica Acta, 2006, 560, 1-23.

[2] C. F. Poole, The essence of chromatography, Elsevier, 2003.

[3] I. Glasgow, J. Batton and N. Aubry, "Electroosmotic mixing in microchannels," Lab Chip, 2004, 4, pp. 558-562.

[4] C. C. Chang, R. J. Yang, "Electrokinetic mixing in microfluidic systems," Microfluid Nanofluid, 2007, 3, pp. 501–525.

[5] T. Sun, N.G. Green, S. Gawad and H. Morgan, "Analytical electric field and sensitivity analysis for two microfluidic impedance cytometer designs," IET Nanobiotechnol., 2007, 1, (5), pp. 69–79.

[6] X. Xuan and D. Li, “Electroosmotic flow in microchannels with arbitrary geometry and arbitrary distribution of wall charge”, Journal of Colloid and Interface Science, 2005, 289, 1 , 291-303

[7] Pennathur S, Santiago JG., “Electrokinetic transport in nanochannels. 1. Theory”, Anal Chem., 2005, 1;77, 21, 6772-81

[8] N. L. Jeon, K. W. Dertinger, D. T. Chiu, I. S. Choi, A. D. Stroock, G. M.Whitesides, "Generation of solution and surface gradients using microfluidic systems", Langmuir 16(22), 2000, pp. 8311–8316.

[9] A. Maha, D. O. Barrett, D. E. Nikitopoulos, S. A. Soper, M. C. Murphy, "Simulation and design of micro-mixers for microfluidic devices," in MicroFluidics, BioMEMS, and Medical Microsystems II, 2003.